WPJET1-PR(17) 17823

J Garcia et al.

On the validity of scaling laws for plasma predictions

Preprint of Paper to be submitted for publication in
Plasma Physics and Controlled Fusion

This work has been carried out within the framework of the EUROfusion Consortium and has received funding from the Euratom research and training programme 2014-2018 under grant agreement No 633053. The views and opinions expressed herein do not necessarily reflect those of the European Commission.

On the universality of power laws for tokamak plasma predictions

J. Garcia[a], D. Cambon[a] and JET Contributors*

Eurofusion Consortium JET, Culham Science Centre, Abingdon, OX14 3DB, UK
[a] CEA, IRFM, F-13108 Saint-Paul-lez-Durance, France
* See the author list of "Overview of the JET results in support to ITER" by X. Litaudon et al. to be published in Nuclear Fusion Special issue: overview and summary reports from the 26th Fusion Energy Conference (Kyoto, Japan, 17–22 October 2016)
E-mail: jeronimo.garcia@cea.fr

Abstract
Significant deviations from well established power laws for the thermal energy confinement time, obtained from extensive databases analysis, have been recently reported in dedicated power scans. The validity and universality of power laws as tools for predicting plasma performance is analyzed in this paper in the framework of a simplified modeling for the heat transport which is however able to account for the interplay between turbulence and collinear effects with the input power which reduce turbulence. Whereas at low power usual scaling laws are recovered with little influence of other plasma parameters, at high power it is shown how the exponents obtained are extremely sensitive to the heating deposition, the q-profile or even the sampling or the number and sampling of points considered. In particular circumstances, even a minimum of the thermal energy confinement time with the input power can be obtained, which means that the approach of the energy confinement time as a power law is intrinsically invalid. Therefore, predictions of future plasmas performance using such approach, mainly at high β, can lead to significant deviations from reality and provide misleading results.

Keywords: plasma confinement, scaling laws, heat transport, non-linearity, fast ions

1 Introduction

Performance prediction of magnetically confined plasmas has been a long and outstanding priority in the nuclear fusion field since fusion reactions have been envisaged as a promising source of energy. Several and complementary approaches have been followed to accomplish this goal. One is based on the reproducibility of present day plasmas by means of either empirical or reduced models obtained from first-principle physics (or just using first principle models) able to account for transport (mainly driven by turbulence in the core region) and MHD, which are the main physical processes limiting the thermal energy confinement. A general framework of validation and verification against experimental data is established with these models in order to check their accuracy. An alternative is the prediction of the thermal energy confinement time by assuming power-law dependencies on different dimensionless and dimensional parameters both in the L and H -modes [1,2]. The exponents of such power laws are obtained by analyzing extensive plasma databases from different tokamaks and performing regressions. One of the most important and striking dependencies obtained is the strong power degradation of the thermal energy confinement time, both obtained in L-mode [1] and H-mode [3], including the most commonly used scaling law IPB98(y,2) for which $\tau_E \sim P_{in}^{-\alpha}$ with P_{in} the injected power and $\alpha = -0.69$.

Recently, in dedicated power scans both at JET [4] and DIII-D [5], significant deviations from IPB98(y,2) have been reported. In both cases, lower thermal energy confinement time degradation with the injected power is obtained with respect IPB98(y,2). In the case of JET, gyrokinetic simulations have shown that turbulence driven by Ion Temperature Gradient (ITG) modes dominates those plasmas and it is non-linearly suppressed by the increased electromagnetic effects and fast ions impact which are collinear with the increased Neutral Beam Injection (NBI) power used [6]. Moreover, turbulence reduction by $E \times B$ flow shear has been shown to play a much weaker role. This point has been demonstrated in DIII-D by performing power scans with reduced torque and for which a deviation from IPB98(y,2) is also obtained [5].

In general, the ability of quasi-linear turbulent models for predicting such deviations is far from optimum as they do not include non-linear physics which is supposed to play a significant role. Additionally, there is not a full understanding on the origin of strong deviations from the IPB98(y,2) scaling, as in addition to electromagnetic effects and fast ions, factors collinear with the injected power, as the ratio T_i/T_e, could play a role. Therefore, systematic gyrokinetic analyses of an enormous experimental database would be required in order to improve and guide quasi-linear predictions, however, this would require an enormous computational effort which is not possible in present-day conditions.

In this context, the applicability of power laws for predicting the thermal energy confinement time, although desirable, is doubtful, which is a significant drawback for the evaluation of future tokamak devices as ITER. Some attempts have been carried out in order to improve the calculation of some exponents, for instance, the one related to $\beta = 4\mu_0 P/B^2$ with P the pressure and B the magnetic field, which lead to inconclusive results [7]. Indeed, the creation of a new scaling covering new experiments could be envisaged, but the question about its validity as a mechanism for performing extrapolations, the applicability domain, the universality of the exponents obtained and the link with the underline physics would be still open. In this paper, the interplay between turbulence and power laws, in particular for input power, is analyzed in the framework of a simplified transport model for heat transport which is able to capture the turbulence suppression by collinear effects with the input power, and to reproduce as well the experimental deviations from well established scaling laws. The implications that such interplay may have on the universality and validity of the scaling law approach is therefore clarified.

2 Modeling framework

The steady-state heat transport equation is solved in cylindrical coordinates for JET high triangularity plasmas with a deviation from the IPB98(y,2) scaling described in [4]:

$$-\nabla Q + S(r) = 0 \tag{1}$$

where Q is the heat flux given by:

$$Q = -n\chi\nabla_r T \tag{2}$$

with n the density, χ the diffusivity and T the temperature and $S(r)$ is the power source.

JET configuration parameters from [4] are chosen, being the major radius $R = 3$ m, minor radius $a = 1$ m and the magnetic field $B = 1.75$ T. In order to take into account the plasma elongation, volume integrals are re-normalized to match the JET discharges volume. In those experiments the density profile was nearly unchanged , meaning that the main reason for the deviation from IPB98(y,2) was the heat transport channel. Therefore, here it is assumed a flat density profile for simplicity, with the value of the average density from experiment, $n = 4.10^{19}$ m^{-3}. The heating power deposition is modeled as a Gaussian profile, $S_0 e^{-5r^2}$ and S_0 a variable for adjusting the injection power. This type of profile resembles the NBI heating on-axis deposition obtained in the real experiment. Moreover, for the sake of simplicity, we consider a mono-fluid approach.

The analysis performed in this paper focuses in the plasma core, i.e. we do not simulate the pedestal region. Appropriate boundary conditions will be taken at the plasma edge depending on the simulation performed. These conditions will be clarified in each section. At $r = 0$ it is assumed that $\nabla_r T = 0$.

The model used in this paper for the heat diffusivity follows the general structure of the so called 'stiff models', with a dependence on the temperature gradient and with a critical threshold for the onset of turbulence, and it is based in previous attempts to apply simplified stiff models [8]:

$$\chi = \chi_e q^\nu (\nabla_r T)^\gamma + \chi_o \tag{3}$$

where χ_e is a constant which will be adjusted by fitting JET data, q the safety factor, ν an empirical exponent, χ_0 the background diffusivity due to collisions in the neoclassical approach, and γ a temperature gradient exponent. In this model we do not include a specific threshold as in previous gyrokinetic analyses [6] it has been shown that, for any input power, there is turbulent transport.

3 Analytical analysis

As a first step, a simplified analytical analysis has been carried out by assuming that $\chi_o = 0$. The heat transport equation has been solved with the model shown in equation (1) and a relation between both γ and α has been found. The resulting temperature profile is given by:

$$T(r) - T_a = \int -\left(\frac{1}{n\chi_e q^\nu}\frac{1}{r}\int S(r')r'dr'\right)^{\frac{1}{1+\gamma}} dr \tag{4}$$

T_a is a boundary condition at $r = a$. Then assuming that a power scan is made by keeping the same shape in the power density profile, i.e. $S(r) = S_0 e^{-5r^2}$ and only S_0 changes with the injected power then we have:

$$T(r) - T_a \sim {S_0}^{1/(1+\gamma)} \tag{5}$$

Taking into account that the energy content is:

$$W_{th} = \int_\tau \frac{3}{2} n\, T\, d\tau \tag{6}$$

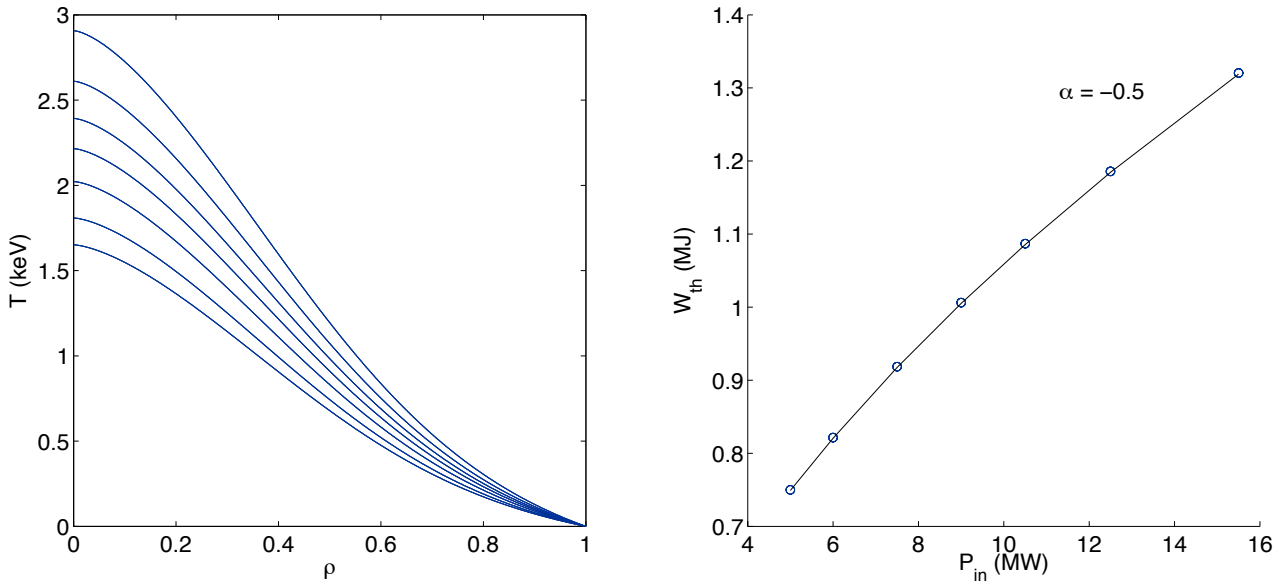

Figure 1: Modelling core temperature profile and core energy as a function of absorbed heating power assuming a model exponent $\gamma = 1$.

with $d\tau$ the volume element, and the heating power is estimated from the source as:

$$P_{in} = \int_{\tau} S(r)\, d\tau \tag{7}$$

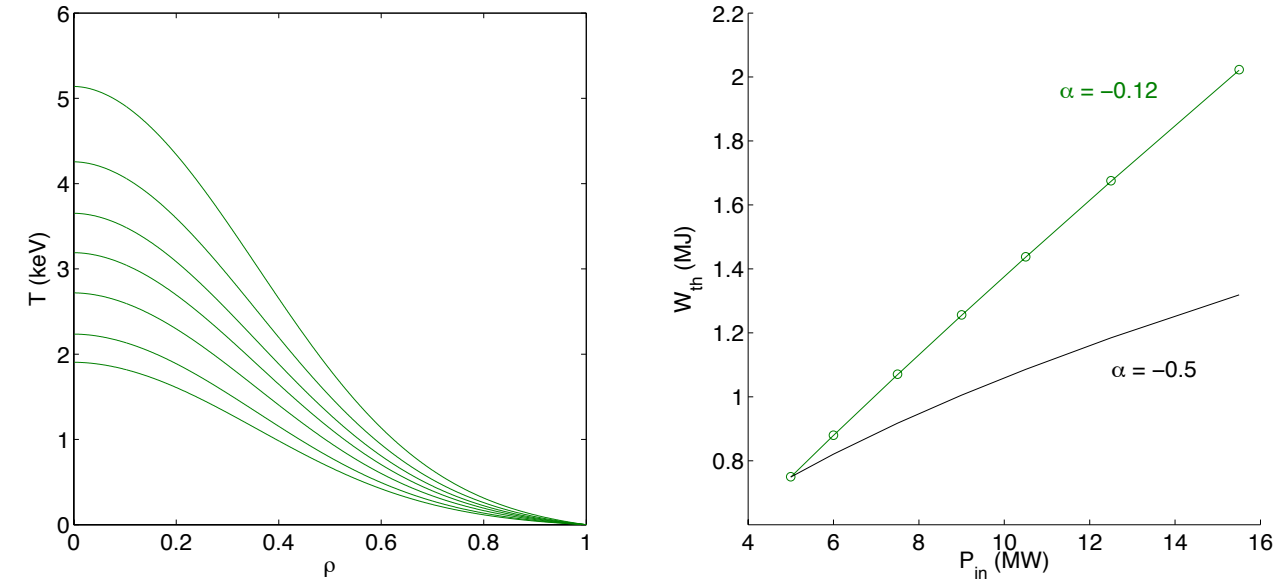

Figure 2: Modelling core temperature profile and core energy as a function of absorbed heating power assuming a model exponent $\gamma = 0.14$.

then by assuming, as it is usually done when creating scaling laws, that the thermal energy is adjusted to the power law:

$$W_{th} \sim P_{in}^{\alpha+1} \tag{8}$$

we obtain, by identifying the exponents, that $\alpha = -\gamma/(\gamma+1)$. If $\gamma = 1$ is assumed, as it is done in typical stiffness studies [8], then $\alpha = -1/2$ is obtained. This is in agreement with the IPB89-P law in L-mode [1]. For JET C-wall high triangularity power scans, $\alpha = -0.5$ is also obtained [4]. In general, for the L-mode $\alpha = -0.6 \pm 0.1$ [9].

Therefore, it would be tempting to proceed in the inverse way by using the exponent α obtained for W_{core} in scans showing a significant deviation from usual scaling laws in order to calculate γ for the model in equation

3 with the aim of analyzing whether a model of the type 3 could reproduce such deviations. This is done for JET-ILW high triangularity plasmas for which $\alpha = -0.12$ was obtained in [4]. $\gamma = 0.14$ is used in 3. Equation 3 is solved for teh two cases considered in this analysis, $\gamma = 1$ and $\gamma = 0.14$, and the results shown in figure 1 and 2. The constant S_0 has been varied in order to cover the range of input power applied in JET power scans [4]. In this simplified modeling T_a has been set to zero for the sake of simplicity. The safety factor, q is assumed to be $q = (0.98 + \rho^{3.14} + (0.74\ \rho)^4)^2$, with ρ the normalized geometrical minor radius, as its shape is close to the one obtained in the experimental power scans and $\nu = 3/2$. The constant χ_e is adjusted in such a way that it matches the core energy content of the lowest input power plasma obtained in JET-ILW high triangularity scan and it is kept fixed as the the constant S_0 is changed. The α exponent is extracted while adjusting the obtained data to the law with expression 8 as it is the case in JET scans. The scaling exponent $\alpha = -0.5$ is obtained when $\gamma = 1$ confirming the analytical results, on the other hand, when using $\gamma = 0.14$ the temperatures obtained are three order of magnitude higher than the experimental ones, showing that this value is unacceptable for simulating these plasmas. A way to solve this is to rescale the heat transport by re-normalizing the constant χ_e again to the experimental energy content. By doing this, as shown in figure 3, the temperatures obtained are in the ballpark of the experimental ones with indeed $\alpha = -0.12$. We therefore arrive to the conclusion that a model like 3, with a fixed structure, should be adapted to each particular trend obtained from dedicated power scans with different α values. Indeed another possibility is to change the constant χ_e, and still keeping $\gamma = 1$, at each input power in order to match the core energy content for each scan. This would mean that the stiffness level changes with power.

In the following sections we propose an alternative model in order to enclose globally both conditions: adhere to well established scaling laws and explain deviations at high power. The differences with models like 3 will be theretofore clarified.

4 Non-linearity with power

Recent gyrokinetic simulations performed for plasmas from the development of the Hybrid scenario in JET C-wall with high confinement have shown that pressure gradients are able to reduce turbulence driven by ITG in electromagnetic simulations, i.e. at high β [10,11]. Similar conclusions have been reached for the JET-ILW power scan discharges with NBI heating and significant deviation form the IPB98(y,2) scaling [6]. These findings suggest that collinear effects with input power, in particular fast ions pressure gradients as they significantly increase pressure gradient without contributing to the turbulence drive in the ITG domain, may affect the underlying turbulence. Additionally, an interplay with the magnetic shear has been also found [11]. Therefore, the model proposed in the equation 3 has been improved by including an extra function F able to capture non-linear contributions from pressure gradients leading to reduced turbulence.

The diffusivity coefficient is defined as 'standard scaling':

$$\chi = \chi_e\ q^\nu\ \nabla_r T\ F(s, \alpha_{MHD,th}, \alpha_{MHD,fast}) + \chi_o \tag{9}$$

where $F(s, \alpha_{MHD,th}, \alpha_{MHD,fast})$ is a function involving three physical parameters: s the magnetic shear, $\alpha_{MHD,th} = -Rq^2 \dfrac{d\beta_{th}}{dr}$, and $\alpha_{MHD,fast} = -Rq^2 \dfrac{d\beta_{fast}}{dr}$, with $\beta_{th} = 4\mu_0 P_{th}/B^2$ and $\beta_{fast} = 4\mu_0 P_{fast}/B^2$.

The F function is:

$$F(s, \alpha_{MHD,th}, \alpha_{MHD,fast}) = \left(1 + 0.5e^{-8(s - \alpha_{MHD,th} - \alpha_{MHD,fast})}\right)^{-1} \tag{10}$$

which has already been studied just including the magnetic shear s in previous analyses of Internal Transport Barrier scenarios for ITER [12]. The generalized magnetic shear $(s - \alpha_{MHD,th} - \alpha_{MHD,fast})$ is introduced containing the fast ions contribution to the pressure gradients. The F function is significantly close to zero when $(s - \alpha_{MHD,th} - \alpha_{MHD,fast})$ becomes also close to zero leading to turbulence suppression.

It is worth clarifying that the factors $\alpha_{MHD,th}$ and $\alpha_{MHD,fast}$ play a different role in this model. Whereas $\alpha_{MHD,th}$ can reduce turbulence it also contributes to the turbulence drive though the factor $\nabla_r T$, however, $\alpha_{MHD,fast}$ just reduces turbulence. In order to model the fast ion contribution term from the NBI heating we make $\beta_{fast} = \chi_{fast} S(r)$ with χ_{fast} a constant to adjust.

Additionally, we have also analyzed an alternative model to the one in equation 9 by including an explicit 'gyroBohm scaling' in the temperature which reads:

$$\chi_{gB} = \chi_{e_{gB}}\ q^\nu\ T^{3/2}\ \frac{\nabla_r T}{T}\ F(s, \alpha_{MHD,th}, \alpha_{MHD,fast}) + \chi_o \tag{11}$$

Modelling results are given and discussed in the following sections.

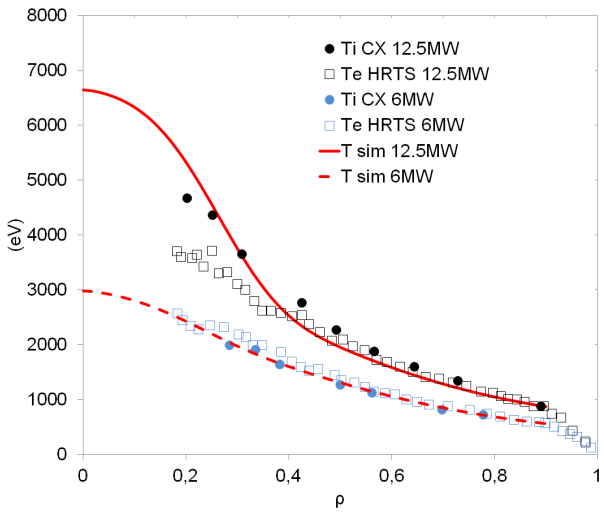

Figure 3: Comparison between core temperature profiles from equation 9 assuming a q-profile $q = (0.98 + \rho^{3.14} + (0.74\ \rho)^4)^2$ for input power points $P_{in} = 6$ MW and $P_{in} = 12.5$ MW and the experimental data obtained for the discharges 84544 and 84545 for the same input powers respectively.

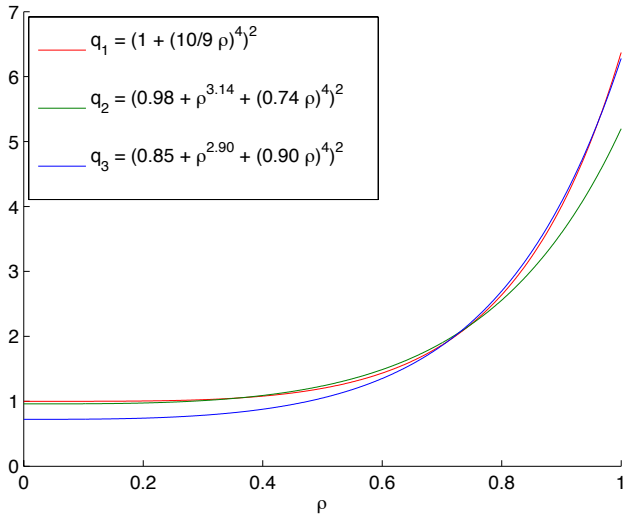

Figure 4: q-profiles at the scaling analysis in each of the power scans.

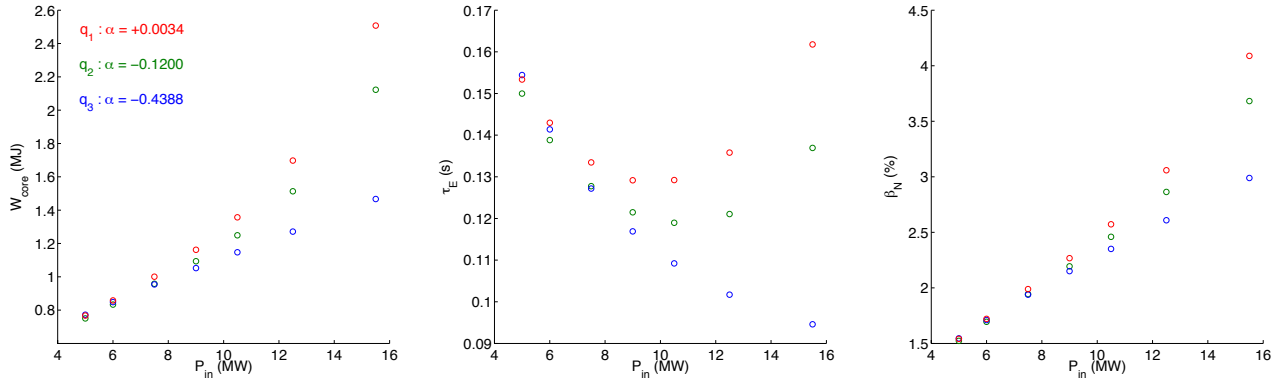

Figure 5: Modelled core energy (left), confinement time (center), and β_N (right) power scans from equation 9 including collinear effects assuming the q-profiles (figure 4) and an on-axis heating profile.

5 Scaling analysis

The previous models are tested against a JET-ILW high triangularity power scan [4] by solving equation 1 with the model 3 for the same input power used in [4]. The boundary condition is taken at the pedestal location and $T_{r_{ped}}$ is adjusted to follow the increasing experimental temperature with the injected power. As performed in section 2, the constant χ_e is adjusted in such a way that it matches the core energy content of the lowest input power plasma, whereas χ_{fast} is adjusted in order to get the experimental exponent from equation 8 which is $\alpha = -0.12$ for the plasmas analyzed. The pedestal energy W_{ped} is removed integrating the energy density profile over the same plasma volume and leading to analyze the core energy W_{core} from the thermal stored energy W_{th} by $W_{core} = W_{th} - W_{ped}$. In order to verify if this approach is correct, the temperature profiles obtained for $P_{in} = 6$ MW and $P_{in} = 12.5$ MW are compared to the experimental ion temperature obtained from Charge-Exchange (CX) measurements and the electron temperature from High Resolution Thomson Scattering (HRTS) averaged over the time window $t = 45.2 - 45.5$ s. As shown in figure 3, the agreement is acceptable with the ion temperature profile with just some slight underestimation at high power in the region $0.4 < \rho < 0.6$ with ρ the normalized geometrical minor radius. This modeling set-up therefore allows for a dedicated analysis of the link between local transport and input power scaling exponents for different experimental conditions. In this case $\chi_o = 0.001$ m^2 s^{-1} has been used, however it does not play a significant role as the turbulence

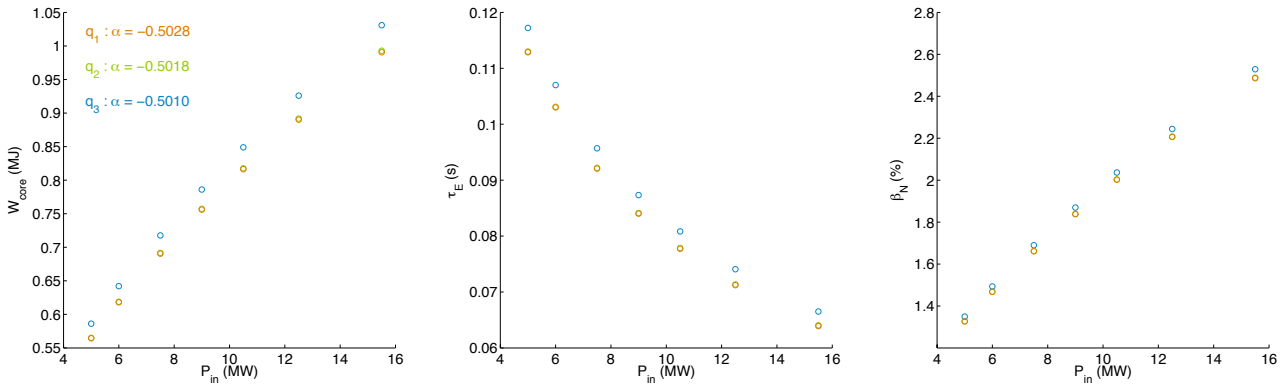

Figure 6: Modelled core energy (left), confinement time (center), and β_N (right) power scans from model 9 including collinear effects assuming the q-profiles (figure 4) and an off-axis heating profile.

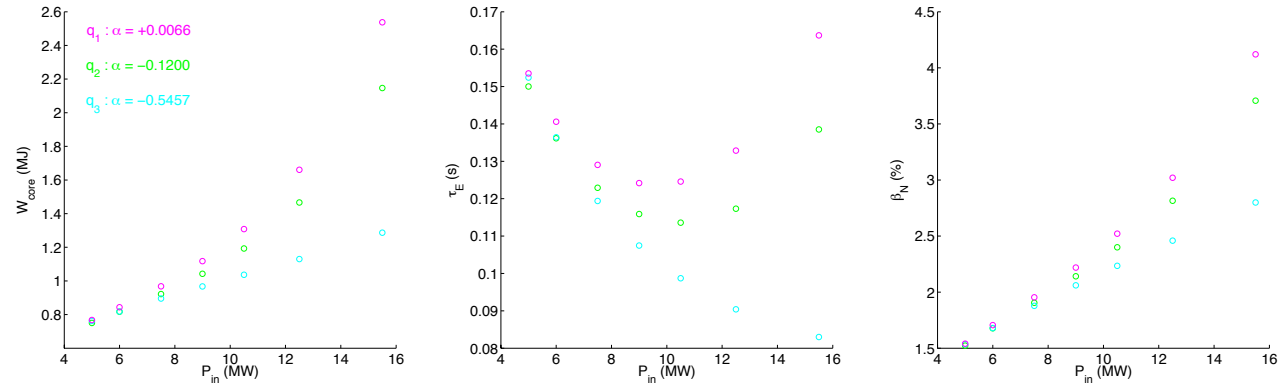

Figure 7: Modeled core energy (left), confinement time (center), and β_N (right) power scans from gyroBohm model in equation 11 including collinear effects assuming the q-profiles (figure 4) and an on-axis heating profile.

transport is always much higher.

A first analysis has been performed by modifying the q-profile assumed with the aim of evaluating the impact of the q-profile typically obtained in different tokamak scenarios. The different q-profiles, which are illustrated in figure 4, $q_1 = (1+(10/9\ \rho)^4)^2$, $q_2 = (0.98+\rho^{3.14}+(0.74\ \rho)^4)^2$, and $q_3 = (0.85+\rho^{2.90}+(0.90\ \rho)^4)^2$, are assumed in order to evaluate the impact of the different magnetic shear in the inner and outer part of the plasma. The scaling exponent α adjusted to the power law in equation 8 is obtained by means of performing the simulation from the transport model with equation 9. Every time a new point is added, the exponent is calculated. The scaling exponent series starts to be calculated when the law has at least three power points. The different α obtained are shown in table 1. At low power, the values of exponent α are close to -0.5 as the pressure gradients are weak and the results from section 2 are recovered. However, at higher power, non-linear effects become stronger and there is a clear deviation among the different q-profiles leading to significant differences in α. One crucial additional result is obtained from this analysis. The scaling exponent α evolves rapidly, for q_1 and q_2, when the power points are close to high input power values around 10 MW, which means that the addition of a few points at high power lead to strong deviations of α. In particular, the highest power point has a strong weight. This shows that the development of scaling laws from experimental results must include the bias at high injection power. The consequences of this behavior for the creation of scaling laws, in particular that for power, will be analyzed in the following sections.

In order to have a deeper insight on the deviation of the exponent α with the power, the energy confinement time τ_E is calculated and plotted against the input power in figure 5 for the different q-profiles used. At low power, τ_E follows a scaling law of the type $\tau_E \sim P_{in}^{-\alpha}$ however at high power, when the non-linearity with power becomes stronger, a minimum on τ_E appears at $P_{in} \sim 10.5$ MW for q_2 and τ_E actually increases with P_{in} beyond that point. With more advanced q-profiles, e.g. with low or even negative magnetic shear in core region, this minimum can appear for lower power inputs, as we can see for q_1 at $P_{in} \sim 10$ MW, which means that it is not a fixed point and it seems to rely on several correlated factors enabling collinear effects (q-profile, heating profile, F-profile, β_{fast}-profile, ...) and needs to be studied in future analysis. This indicates that an approximation of

	Standard scaling			Off-axis heating			GyroBohm scaling		
P_{in} (MW)	q_1	q_2	q_3	q_1	q_2	q_3	q_1	q_2	q_3
5									
6									
7.5	-0.3418	-0.3947	-0.4789	-0.5025	-0.5016	-0.5009	-0.4264	-0.4896	-0.6016
9	-0.2943	-0.3603	-0.4737	-0.5026	-0.5017	-0.5009	-0.3638	-0.4416	-0.5949
10.5	-0.2384	-0.3183	-0.4676	-0.5027	-0.5017	-0.5010	-0.2911	-0.3832	-0.5867
12.5	-0.1518	-0.2502	-0.4579	-0.5027	-0.5018	-0.5010	-0.1812	-0.2901	-0.5731
15.5	+0.0034	-0.1200	-0.4388	-0.5028	-0.5018	-0.5010	+0.0066	-0.1200	-0.5457
5									
5.25									
5.5	-0.3963	-0.4326	-0.4851	-0.5023	-0.5015	-0.5007	-0.4982	-0.5417	-0.6092
5.75	-0.3906	-0.4286	-0.4844	-0.5023	-0.5015	-0.5008	-0.4906	-0.5364	-0.6084
6	-0.3846	-0.4246	-0.4838	-0.5024	-0.5015	-0.5008	-0.4828	-0.5308	-0.6076
10	-0.2409	-0.3205	-0.4680	-0.5027	-0.5017	-0.5010	-0.2942	-0.3861	-0.5871
15.5	+0.0125	-0.1104	-0.4374	-0.5028	-0.5017	-0.5010	+0.0156	-0.1091	-0.5434
5									
10									
14.5	-0.0466	-0.1608	-0.4450	-0.5027	-0.5018	-0.5010	-0.0546	-0.1733	-0.5545
14.75	-0.0049	-0.1263	-0.4400	-0.5027	-0.5018	-0.5010	-0.0035	-0.1271	-0.5473
15	+0.0184	-0.1067	-0.4371	-0.5027	-0.5018	-0.5010	+0.0247	-0.1022	-0.5432
15.25	+0.0363	-0.0916	-0.4349	-0.5027	-0.5018	-0.5010	+0.0460	-0.0827	-0.5399
15.5	+0.0520	-0.0781	-0.4329	-0.5027	-0.5018	-0.5010	+0.0647	-0.0654	-0.5370

Table 1: Scaling table.

the type $\tau_E \sim P_{in}^{-\alpha}$, which is used for fitting plasmas with different origins, and with a fixed α, supposed to be universal for the sake of extrapolation, is not applicable when there are extra effects affecting turbulence and which are collinear with the injected power. On the other hand, that approximation can be used at low power. In order to clarify the range of applicability in inter machine comparisons, the dependence of a normalized and dimensionless parameter as β_N is more helpful. In figure 5, the dependence of β_N (calculated including the pedestal region in this case) with the injected power is shown. The existence of a minimum of τ_E seems to be linked to crossing $\beta_N \sim 2.5$ which is a rather high value, and in the case of JET, Neoclassical Tearing Modes's (NTM) can be quite deleterious for the q-profiles considered in this paper [13]. Therefore, a clear experimental demonstration of the existence of this minimum can be difficult, however, significant deviations from well established scaling laws should be noticeable when approaching that minimum. An alternative scan has been performed by changing the input power location (but keeping the total input power constant), i.e. assuming a heating profile $S_0 e^{-5(r-0.5)^2}$. The results obtained for the different q-profiles are shown in figure 6. In this case, the exponent α is nearly identical for the different profiles and the deviation at high power just disappears. As shown in table 1 as well, the addition of each point does not lead to significant changes on α. This indicates that different heating profiles can lead to significant deviations on α obtained.

In the case of the gyroBohm scaling, same q-profiles and on-axis heating profile are assumed and the heating range is unchanged. New constants $\chi_{e,gB}$ and $\chi_{fast,gB}$ are adjusted expecting to obtain the last exponent $\alpha = -0.12$. The results are presented in figure 7. Concerning the confinement time, as it happened with equation 9, a minimum appears at $P_{in} \sim 10$ MW. Hence the same remarks apply, therefore the type $\tau_E \sim P_{in}^{-\alpha}$ law is still not a good representation of the experiments.

6 Impact of sampling

The fact that points with different levels of power weight in a different way when calculating the exponent α has important consequences when a power law is created from a significant number of experimental discharges at different power levels. This is specially important for determining scaling from databases as they tend to include an unbalanced quantity of pulses with more pulses at low power (and low beta). Moreover, even if the pulses used could have the same input power, some non-linear physics collinear with the power could be different (for instance, by using different heating mechanisms), which could lead to a systematic difference. In order to illustrate this, the following numerical experiment has been carried out.

Firstly, we analyzed how the distribution of the power input points could affect the calculation of the α exponent. The first power distribution corresponds to that used for calculating the results shown in figures 5, 6 and 7 respectively. Two other distributions are studied: the second one uses a higher density of points at very

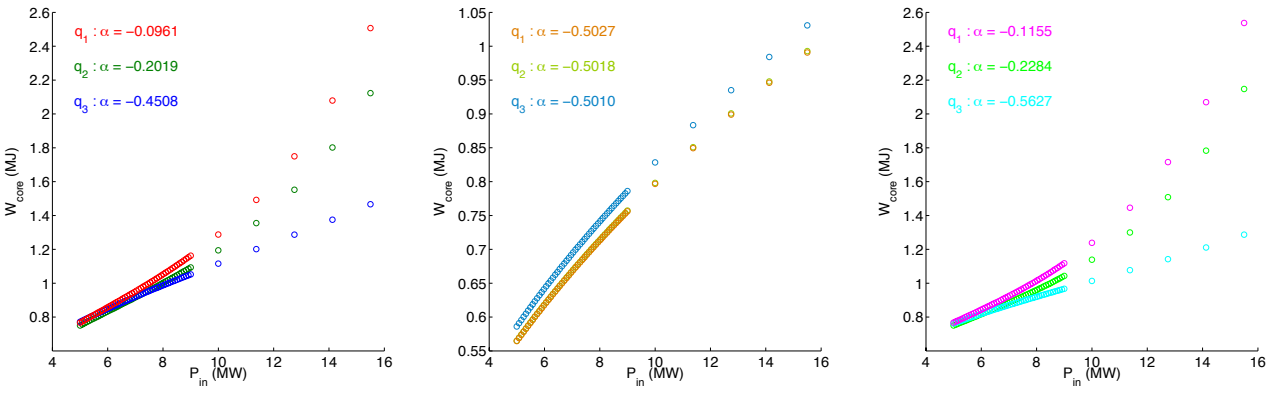

Figure 8: Modelled core energy power scans for a standard scaling (left), off-axis scaling (center), and gyroBohm scaling (right) assuming the q-profiles (figure 4) and 50 points inputs at low power.

low power around 5 MW; the third one uses a higher density of points at very high power around 15 MW. This analysis is done for the three q-profiles considered in this paper.

In general, the exponents found have a significant variance around the standard distribution of points used in the previous section. This is particularly true for the cases with q_1 and q_2. Regarding the second distribution, the last $\alpha = -0.1104$ goes beyond the reference $\alpha = -0.12$ because the interpolation is directly calculated between lower points and just a high power point. The third distribution shows that higher power points have stronger weight as $\alpha = -0.0781$, as a result of the amplification of the collinear effects at this specific range. This scattering of α results is more pronounced for q_1 and almost nonexistent for q_3 where the sames results are obtained regardless the distribution of points.

For the off-axis power deposition case, no matter how the points are distributed, the values of α are homogenous and they do not show any dependence on the distribution of points. The gyroBohm case shares the same behavior with the standard case in every distribution, however a higher range of α is obtained, from $\alpha \approx -0.6$ at low power up to $\alpha \approx +0.06$ at high power.

Secondly, we increased the number of points and assumed a specific distribution, shown in figure 8, with the aim of evaluating how the number of points affects the α exponent progression. The range contains fifty points between 5 MW and 9 MW and 5 points between 10 MW and 15.5 MW. Same q-profiles are used to analyze their impact. Concerning the results with equation 9, something relevant to note is the last point at 15.5 MW obtains a different $\alpha = -0.2019$ compared to the value $\alpha = -0.12$ (table 1) and it seems that increasing the number of points at low power leads to a decreasing of α exponent evolution at high power. This is quite important as it is usually easier to have discharges at low power than at high power where additional problems (as MHD activity) can reduce the plasma stability. Based on the results shown here, this means that, with unbalanced number or points, predicting the performance of high β plasmas by means of scaling laws can lead to significant under predictions of performance.

7 Local transport analysis

A transport analysis has been carried out in order to further investigate the physical implications, from the transport point of view, of the deviations from well established scaling laws. A particular focus is put on the so-called 'stiffness', which can be considered as the derivative of the diffusivity with respect to the gradient $\partial\chi/\partial(\nabla T)$. For models like the ones described in equation (3) the stiffness is χ_e.

A local transport analysis has been performed based on the model described by the proposed diffusivity in equation 9. Therefore, the flux is calculated based on equation 2. We undertake the same conditions than in previous sections. In each simulation,the same q-profiles shown in figure 4 have been assumed. The power source is on-axis. The input power points range from 4 to 15 MW. The analysis will be done locally for $\rho = 0.4$ and $\rho = 0.7$, as representative of inner and outer core regions respectively.

As shown in figure 9, at low power, when there are not significant deviations from usual scalings, the flux increases with the gradient ∇T both at $\rho = 0.4$ and $\rho = 0.7$ for the three q-profiles considered. Due to the strong increase of flux with the temperature gradient we could consider this behaviour as typically 'stiff'. Going further, the model predicts a saturation of the flux with high power injection at $\rho = 0.4$ for q_1 and q_2, precisely the q-profiles for which a minimum of the confinement time was obtained. This saturation allows for a higher temperature gradient for the same flux. On the other hand, for q_3 there is no saturation. Surprisingly, after passing a maximum point, as long as the flux is saturating, the diffusivity decreases when increasing ∇T at

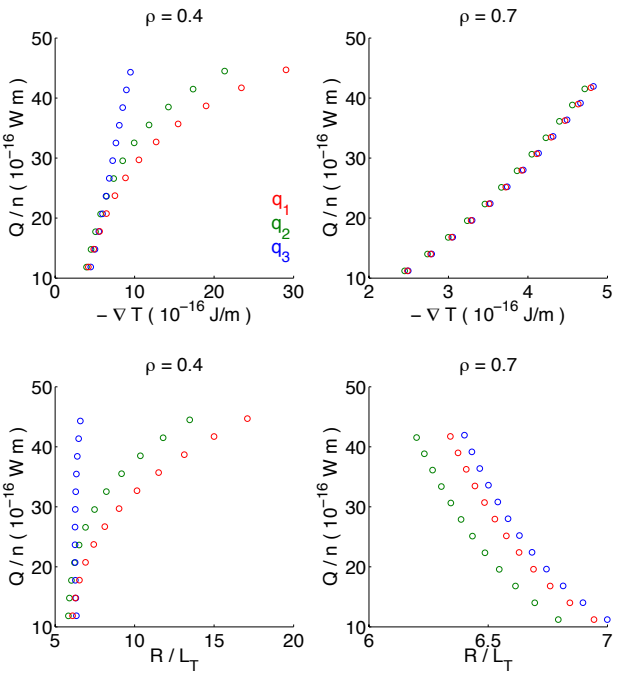

Figure 9: Modelling normalized flux Q/n dependence on ∇T (top) and R/L_T (bottom) in two positions, inner radius $\rho = 0.4$ (left) and outer radius $\rho = 0.7$ (right).

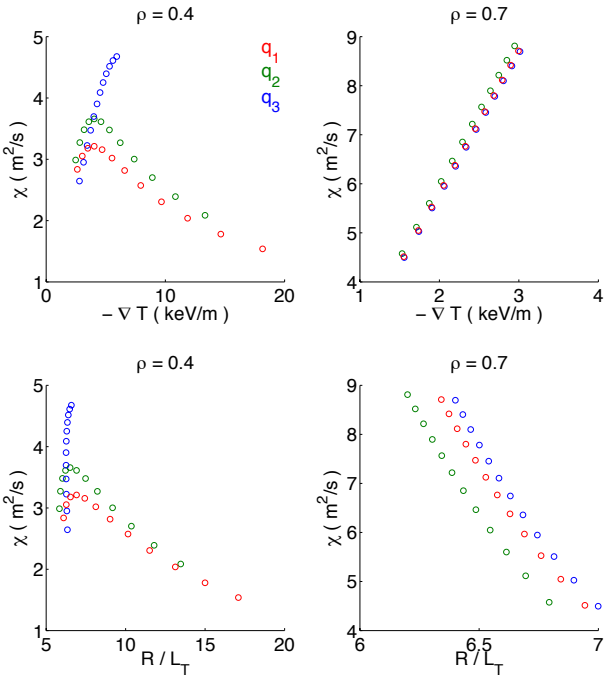

Figure 10: Modelling diffusivity χ dependence on ∇T (top) and R/L_T (bottom) in two positions, inner radius $\rho = 0.4$ (left) and outer radius $\rho = 0.7$ (right).

$\rho = 0.4$ whereas the trend is the opposite at $\rho = 0.7$ as shown in figure 10. A similar analysis has been performed by using the more standard normalization R/L_T with $L_T = T/\nabla_r T$. The usual concept of stiffness is very clear from figure 10 where χ_e is clamped at $R/L_T = 6$ at $\rho = 0.4$ for q_3, regardless the input power applied, and partially for q_1 and q_2 at low power. However, when the power is increased, a maximum of χ_e appears for q_1 and q_2 and then χ_e decreases with increasing R/L_T (increasing power). When performing the same type of analysis with the gyroBohm case, the trend is similar as shown in figures 11 and 12.

It is worth clarifying that such behavior would be impossible to obtain assuming a model based on equation 3 and with constant χ_e, regardless the value of γ.

The previous results are also in agreement with recent power scans performed in DIII-D with NBI heating, which showed a decreasing ion thermal diffusivity with increasing temperature gradient [5] and an ion heat flux saturation in the inner core plasma. This behavior seems counter intuitive as in dedicated stiffness studies the slope of the heat flux as a function of the temperature gradient (or normalized temperature gradient) is clearly positive even in those conditions where a significant turbulence reduction appears [14]. However, it should be pointed out that there are clear differences in the way stiffness experiments and power scans are performed. In stiffness experiments, the local dependence of heat flux and temperature gradients are studied by forcing the plasma to remain at constant temperature in a particular location when the input power is changed with the aim of analyzing $\partial Q/\partial(\nabla T)$. This is done by changing the input power location for the different points analyzed. On the other hand, the heat flux dependence on temperature gradients shed light on the total derivative $dQ/d(\nabla T)$. The first approach is useful for comparing experiments and transport models including temperature gradient dependence (or gyrokinetic simulations) whereas the second one is essential for understanding energy confinement.

8 Pedestal influence

The influence of the pedestal has been also analyzed in a simplified way with the aim of studying separately the impact of the core and edge regions in the deviation from IPB98(y,2) scaling. For that purpose the total thermal energy, W_{th}, and τ_E have been calculated for the results obtained in figures 5 and 7 and the exponent α calculated. The results are shown in figure 13. For all the cases considered there is a significant deviation from IPB98(y,2), for which $\alpha = -0.69$, being the deviation stronger for the cases which showed a minimum of τ_E for the core part, i.e. for q1 and q2. Although there is some difference between the standard and gyroBohm scaling, the trend is quite similar. Interestingly, τ_E has also a minimum for q1 and q2 as it happened in the analysis of W_{core}, indicating that the same remarks discussed in previous sections for the core part can be applied to the

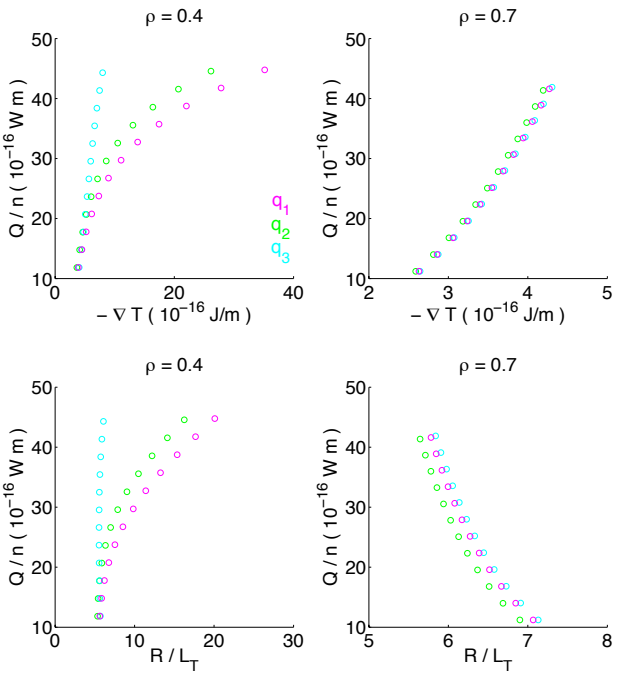

Figure 11: Modelling gyroBohm normalized flux Q/n dependence on ∇T (top) and R/L_T (bottom) in two positions, inner radius $\rho = 0.4$ (left) and outer radius $\rho = 0.7$ (right).

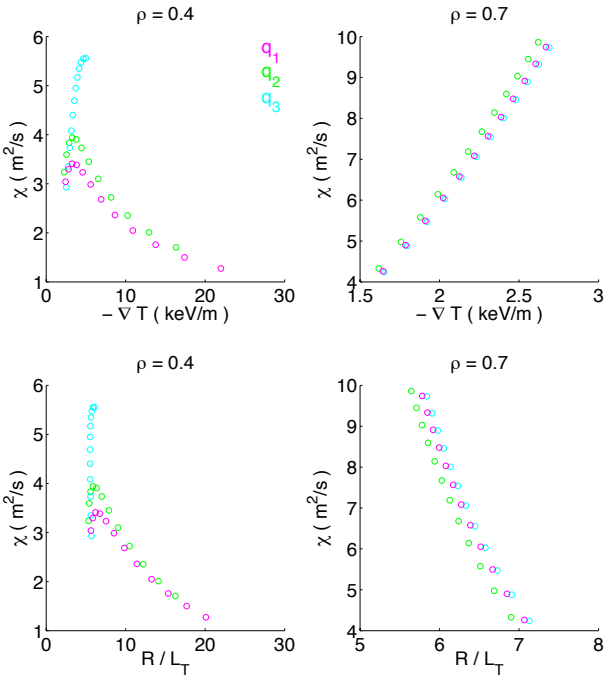

Figure 12: Modelling gyroBohm diffusivity χ dependence on ∇T (top) and R/L_T (bottom) in two positions, inner radius $\rho = 0.4$ (left) and outer radius $\rho = 0.7$ (right).

whole plasma analysis.

However, it is important to stress that, in these simulations, the temperature at the boundary location increases with power following the trend obtained in the experiment and this can have some effect on W_{th} as a pedestal contribution. Therefore, in order isolate this contribution, an alternative simulation has been performed by keeping the temperature constant at the value obtained for $P_{in} = 5MW$, i.e. 500eV, for all the input powers. In the results, shown in figure 14, a much closer agreement to IPB98(y,2) is obtained for q3 both for the standard scaling, $\alpha = -0.66$ and even exact for the one with a gyroBohm dependence, $\alpha = -0.69$. On the other hand, for q1 and q2, still a significant deviation from IPB98(y,2) is obtained due to the low power degradation in the core region. This shows that deviations from IPB98(y,2) are due to combined effects from core and edge regions (or to some interplay not considered here) and that the construction of scaling laws is limited due to the non-linear physics responsible of such deviations.

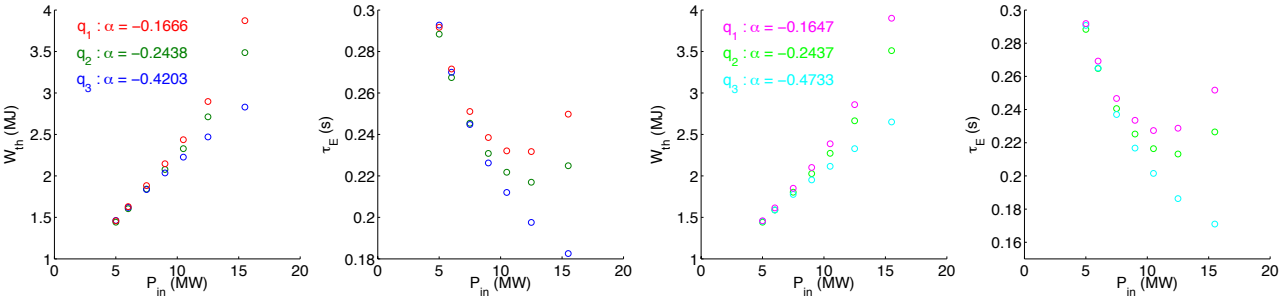

Figure 13: Modelled total thermal energy and confinement time obtained for the standard model from equation 9 (left), and from equation 11 (right) for the power scans shown in figures 5 and 7 respectively.

9 Summary and Conclusions

The link between local transport and global confinement has been studied in the framework of a simplified model which is able to capture the reduction of turbulence by means of combinations of low magnetic shear and high pressure gradients, mainly coming from the fast ion contribution. The model has been tested against power

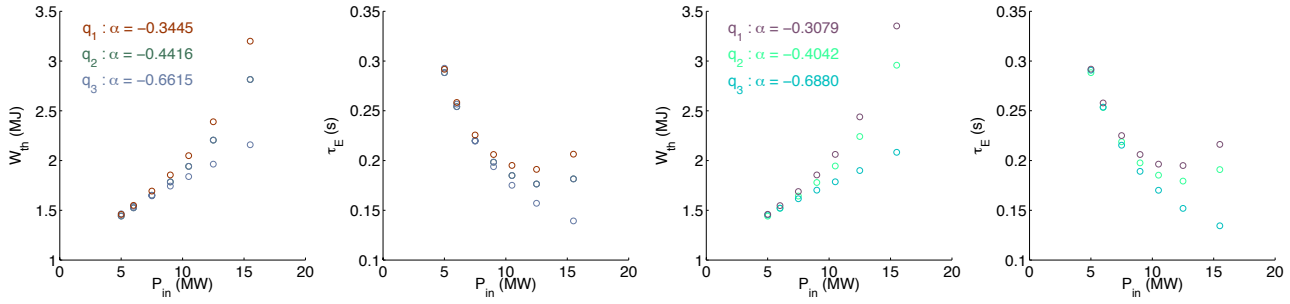

Figure 14: Modelled total thermal energy and confinement time obtained for the standard model from equation 9 (left), and from equation 11 (right) for the power scans shown in figures 5 and 7 respectively.

scans at JET with and without significant deviations from the IPB98(y,2) scaling. When collinear effects with the input power are weak, a power law approximation to the core thermal energy confinement time of the type $\tau_E \sim P_{in}^{-\alpha}$ seems to be a good approach for predicting thermal energy confinement. On the other hand, when the collinear effects are strong at high power, a power law approximation with a constant exponent covering a broad range of powers, can lead to misleading results due to the different weight for the calculation of α of the input power applied. In this case small variations of input power can lead to very significant variations of α. This is particularly shown by performing different sampling of input power points covering the same power range. Depending on where the points are located and their quantity, the exponent α obtained is different, which is a significant drawback as, in general, getting points in different engineering parameters regions can be constrained by inherent limitations, such as MHD activity. The collinear effects with power lead to the appearance of a minimum of the core energy confinement time which indeed invalidates any approximation of the type $\tau_E \sim P_{in}^{-\alpha}$. This minimum is linked to the saturation of core heat flux and the reduction of diffusivity with power and temperature gradient, in agreement with recent power scans at DIII-D. It is worth pointing out that turbulence is not fully suppressed in these conditions. i.e. the plasma does not have an Internal Transport Barrier with just neoclassical transport.

The results from this paper have strong implications for predictions of performance of future tokamak devices by using scaling laws approximations. Using a fixed exponent for the input power, obtained from a regression of a significant number of experimental results from different devices, with a large range of q, fast ion pressure or heating profiles, can lead to significant deviations from real plasma confinement, as this exponent actually depends as well on thermal energy confinement and therefore on the power applied. The IPB98(y,2) scaling, and in general any power law scaling, could still be applied in conditions with weak coupling between confinement and input power, typically at low β, however at high β this approximation cannot be used. One possibility to overcome this issue is calculating exponents in different power regimes which could be identified by different β_N. This possibility will be explored in the future.

Acknowledgements. This work has been carried out within the framework of the EUROfusion Consortium and has received funding from the Euratom research and training programme 2014-2018 under grant agreement No 633053. The views and opinions expressed herein do not necessarily reflect those of the European Commission

References

[1] Yushmanov P. N. *et al Nucl. Fusion* 30, 1999 (1990)
[2] Luce T. *et al Plasma Phys. Control. Fusion* 50 (2008) 043001
[3] ITER Physics Basis, Nucl. Fusion 39, 2175 (1999).
[4] Challis C. *et al Nucl. Fusion* 55 (2015) 053031
[5] Luce T. C. *et al* I1.103 43rd EPS Conference on Plasma Physics, Leuven, Belgium (2016)
[6] Doerk H. *et al Plasma Phys. Control. Fusion* 58 (2016) 115005
[7] Cordey et al, J.G. Nucl. Fusion 45 (2005) 1078–1084
[8] Garbet X. *et al Plasma Phys. Control. Fusion* 46 (2004) 1351–1373
[9] Kaye S.M. *et al* Nucl. Fusion 37 (1997) 1303 .
[10] Garcia J. *et al Nucl. Fusion* 55 (2015) 053007
[11] Citrin J. *et al Plasma Phys. Control. Fusion* 57 (2015) 014032
[12] Garcia J. *et al Phys. Rev. Lett.* 100 (2008) 255004
[13] Hobirk J. *et al Plasma Phys. Control. Fusion* 54 (2012) 095001
[14] Mantica P. *et al Phys. Rev. Lett.* 107 (2011) 135004